Publishing House
AKAPIT

COMPUTER METHODS IN MATERIALS SCIENCE

Informatyka w Technologii Materiałów

Vol. 8, 2008, No. 4

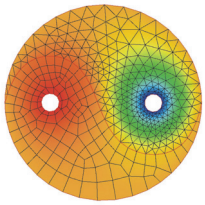

THREE-DIMENSIONAL UPPER BOUND ANALYSES FOR EXTRUSION FROM SQUARE BILLETS THROUGH COMPLEX DIE-OPENINGS' SHAPES

JOSEPH S. AJIBOYE

Department of Mechanical Engineering, University of Lagos, Lagos, Nigeria;
present address: KAIST Valufacture Institute of Mechanical Engineering, School of Mechanical, Aerospace & Systems Engineering, Korea Advanced Institute of Science and Technology
Daejeon 305-701, Korea
E-mail: joesehinde@yahoo.com

Abstract

A numerical model based on the upper bound elemental technique for prediction of extrusion pressure in three-dimensional direct extrusion process is presented. Using square billets, the study of the effect of die land length has been extended to the evaluations of the extrusion pressures to extrude complex sections such as square, rectangular, I, and T shaped sections with power of deformation due to ironing effect at the die land taken into account. The extrusion pressure contributions due to the die land evaluated theoretically for shaped sections considered are found to increase with die land lengths for any given percentage reduction and also increase with increasing percentage die reductions at any given die land length. The effect of die land lengths on the extrusion pressures increase with increasing complexity of die openings geometry with I-shaped section giving the highest extrusion pressure followed by T-shaped section, rectangular, circular shaped die openings with square section die opening, giving the least extrusion pressure for any given die reduction at any given die land length. The proper choice of die land length is, therefore, imperative if excessive pressure buildup at the emergent section is to be avoided so as to maintain the quality and metallurgical structure of the product. Comparison of the least upper bounds extrusion pressures computed with the experimental results and SERR analysis shows that the upper bound method predicts reasonable extrusion loads well within engineering accuracy.

Key words: extrusion pressures, die land, shaped sections, % reduction in area, area ratio, upper bound

1. INTRODUCTION

Upper bound analysis of three-dimensional metal forming processes in general and extrusion in particular has remained a subject of continuum focus of study due to its high productivity, lower cost and increased properties. There are several analytical approaches available to metal forming problems, including slip-line field theory, upper bound and lower bound analyses and finite element methods. Although the FEM provides a more accurate description of the deformation and stresses than do other methods, it demands an expert's use of a lot of computer time. The upper bound approach has much to recommend it, since, it is simple, takes less computer time and expertise, and the results obtained are within reasonable engineering approximations. As regards the three-dimensional extrusion of shaped sections, some analytical methods for predicting the metal flow according to the optimum die configurations have been proposed by some workers (Sahoo & Kar, 2000; Yang & Lee, 1993; Wu & Hsu, 2000; Kim et al., 1999; Kim et al., 2000). Kiuchi et al. (1981) developed an upper bound based analytical method to calculate power requirements, the extrusion pressure, the optimal die length in extrud-

 ISSN 1641-8581

ing/drawing from round, square and rectangular billets to rods, bars and wires with square, rectangular, hexagonal, L-type, T-type, H-type and flower-type cross-sections. For this generalized formulation, it also has the setback for neglecting to account for the frictional forces at the die land region. Nanhai et al. (2000) stressed the importance of proper simulation of die land in the extrusion of shapes with flat-faced die so as to avoid the generations of geometrical defects and hence proposed a method of simulation, using finite element method, that the metal flow in extrusion and the die land can be adjusted according to the simulation results. Ajiboye and Adeyemi (2006) improved on Kiuchi et al. (1981) formulations to account for power losses due to ironing effect at the die land of an extrusion die with circular die opening. Chitkara and Celik (2001) developed, based on upper bound theory, a three-dimensional extrusion of non-symmetric T-shaped sections from initially round billets. Extensive literatures search revealed that, most of FEM simulations (Duan et al., 2004; Venkata et al., 1995; Li et al., 2001; Abrinia & Makaremi, 2008; Filice et al., 2008; Kiuchi et al., 1996; Sheppard & Paterson, 1982) were not on extrusion from square billet to other shaped sections. Kar and Das (1997) reformulated SERR technique so that it could be applied to analyze extrusion of bars of any cross section from billets of any other cross section when the product and billet boundaries were defined by planar surfaces. The effect of percentage reduction in area and the die land length is seen to be more pronounced experimentally in I-shaped section than in T-shaped section. Chitkara and Adeyemi (1997) investigated the effect of percentage reduction in area on the extrusion pressures of I and T-shaped die openings with extrusion pressures of I-shaped section being higher than for T-shaped section opening. All the above mentioned authors limited their working materials to round billets except Kar and Das (1997) and all excluded die land or straight portion of die. There is, to the best of author's knowledge, no research work so far that has either been presented or done on the three-dimensional extrusion of complex shapes using UBET with the powers of deformations due to ironing effect at die land taken into account.

In the present study, three-dimensional analysis for the extrusion of circular and complex sections such as square, rectangular, I- and T-shaped sections from initially square/rectangular billets is studied and presented.

2. THEORETICAL ANALYSIS

2.1. Shape and dimension of die surface

Figures 1(a) and 1(b) respectively show the schematic diagrams of the die surface and shape plus dimensions of the linearly converging die, in Cartesian coordinates system used for the present numerical calculations. In the present modeling, the surface in Cartesian coordinates system is represented by $z_s(x, y)$. In Cartesian co-ordinates system, the die surface (Kiuchi et al., 1981; Ajiboye, 2006) is derived using linearly converging straight lines as:

$$z_s(x,y) = \frac{z_f(y) - z_i(y)}{x_f(y)} x + z_i(y) \qquad (1)$$

where:

$$z_f(y) = (z_i - z_o)\frac{y}{y_1} + z_o,$$

$$z_i(y) = (z_2 - z_o)\frac{y}{y_1} + z_o,$$

$$x_f(y) = (x_i - x_o)\frac{y}{y_1} + x_o$$

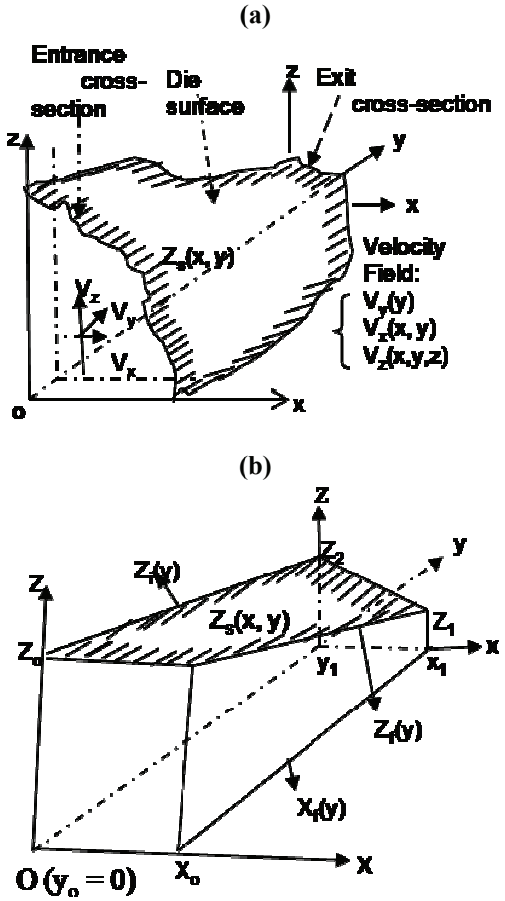

Fig. 1. (a) Schematic diagram of the die surface in Cartesian co-ordinate system Fig. 1 (b) Shape and dimensions of linearly converging die

where x_1, x_o and z_i, z_o are the dimensions of die and billet respectively and y_1 is the length of the die. By using equation (1), and the function $z_s(x, y)$ all of the strain rate components and the total powers of deformation can be calculated.

The boundary limits for the die surfaces are

$$\begin{aligned} 0 \le x \le x_f(y) \\ 0 \le z \le z_s(x,y) \\ 0 \le y \le y_1 \end{aligned} \tag{2}$$

2.1.1. Assumptions

The following assumptions (Ajiboye, 2006) are used;

i) the longitudinal velocity, V_y, is uniform at each cross-section of the material in the die and is equal to inlet velocity denoted by V_o at the entry.
ii) The Von-Mises yield criterion is assumed to be applicable.

The generalized formulas of the kinematically admissible velocity field can be formulated as follows. At first, the condition of volume constancy may be expressed as

$$\dot{\varepsilon}_x + \dot{\varepsilon}_y + \dot{\varepsilon}_z = 0 \tag{3a}$$

that is,

$$\frac{\partial}{\partial x}V_x(x,y,z) + \frac{\partial}{\partial y}V_y(x,y,z) + \frac{\partial}{\partial z}V_z(x,y,z) = 0 \tag{3b}$$

From here, the kinematically admissible velocity fields are derived to be (Ajiboye, 2006)

$$V_y(y) = \frac{V_o \int_0^{x_f(0)} z_s(x,0)dx}{\int_0^{x_f(y)} z_s(x,y)dx} \tag{4}$$

$$V_x(x,y) = \frac{-1}{z_s(x,y)} \int_0^x \frac{\partial}{\partial y}\left[V_y(y).z_s(x,y)\right]dx \tag{5}$$

$$V_z(x,y,z) = -\int_0^z \left[\frac{\partial}{\partial x}V_x(x,y) + \frac{\partial}{\partial y}V_y(y)\right]dz =$$

$$-z\left[\frac{\partial}{\partial x}V_x(x,y) + \frac{\partial}{\partial y}V_y(y)\right] \tag{6}$$

Equations (4), (5) and (6) satisfy the condition of volume constancy and all of the kinematic boundary conditions.

3. STRAIN RATES' COMPONENTS

The strain rates components are the derivatives of kinematically admissible velocity fields of equations (4), (5) and (6). Now, differentiating velocity equation (5) to get strain rate along x-axis i.e,

$$\dot{\epsilon}_{xx}(x,y) = \frac{\partial}{\partial x}V_x(x,y) =$$

$$-\frac{\frac{\partial}{\partial x}z_s(x,y)}{z_s(x,y)}V_x(x,y) - \frac{\partial}{\partial y}V_y(y) - \frac{\frac{\partial}{\partial y}z_s(x,y)}{z_s(x,y)}V_y(y) \tag{7}$$

The strain rate components along y-axis is obtained by differentiating the kinematically admissible velocity field equation (4), i.e,

$$\dot{\epsilon}_{yy}(y) = \frac{\partial}{\partial y}V_y(y) =$$

$$-V_o \int_0^{x_f(0)} z_s(x,y)dx \frac{z_s(x_f(y),y)\frac{\partial}{\partial y}x_f(y) + \int_0^{x_f(y)} \frac{\partial}{\partial y}z_s(x,y)}{\left[\int_0^{x_f(y)} z_s(x,y)dx\right]^2} dy \tag{8}$$

From equations (7) and (8), the strain rate along z-axis, $\epsilon_{zz}(x,y)$ is obtained as:

$$\dot{\epsilon}_{zz}(x,y) = -\left[\frac{\partial}{\partial x}V_x(x,y) + \frac{\partial}{\partial y}V_y(y)\right] \tag{9}$$

The other components of strain rates are defined as follows;

$$\epsilon_{zx}(x,y,z) = \frac{-z}{2}.\frac{\partial^2}{\partial x^2}V_x(x,y) \tag{10}$$

$$\epsilon_{xy}(x,y) = \frac{1}{2}.\frac{\partial}{\partial y}V_x(x,y) \tag{11}$$

$$\epsilon_{yz}(x,y,z) = \frac{-z}{2}\left[\frac{\partial^2}{\partial y \partial x}V_x(x,y) + \frac{\partial^2}{\partial y^2}V_y(y)\right] \tag{12}$$

4. THE UPPER BOUND SOLUTION

The total power consumption, J^*, during extrusion through the die is the sum of the power losses due to the plastic deformation inside the die, (E_i), due to velocity discontinuities (E_s), and that due to frictional resistance at the interface between the material and the die, (E_f). The upper bound on total

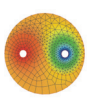

power dissipated is expressed as the sum of the individual term for internal power, shear power and the power to overcome prescribed surface tractions.

$$J^* = \dot{E}_i + \sum_n \dot{E}_s + \sum_k \dot{E}_f \qquad (13)$$

where

$E_i = \frac{2\bar{\sigma}_m}{\sqrt{3}} \iiint_v \sqrt{\frac{1}{2}\dot{\varepsilon}_{ij}\dot{\varepsilon}_{ij}}dV$, i.e.

$$\dot{E}_i = \sigma_o \int\int\int \sqrt{\frac{2}{3}\left\{\dot{\epsilon}_{xx}^2 + \dot{\epsilon}_{yy}^2 + \dot{\epsilon}_{zz}^2 + 2\left(\dot{\epsilon}_{xy}^2 + \dot{\epsilon}_{yz}^2 + \dot{\epsilon}_{zx}^2\right)\right\}} dxdydz \qquad (14)$$

$$\dot{E}_s = \int_{\Gamma_s} \frac{\sigma_o}{\sqrt{3}} (\Delta V)_{\Gamma_s} dS$$

where

$$(\Delta V)_{\Gamma_s} = \sqrt{V_x^2\left(x, y^*\right) + V_z^2\left(x, y^*, z\right)} \qquad (15)$$

$\dot{E}_s = \eta \int_{\Gamma_s} \frac{\sigma_o}{\sqrt{3}} (\Delta V)_{\Gamma_s} dS$ where η = shape constant,

$$(\Delta V)_{\Gamma_s} = \left[V_z\left(x^* + 0, y, z\right) - V_z\left(x^* - 0, y, z\right)\right] \qquad (16)$$

$\sum_k \dot{E}_f = \dot{E}_{m/p} + \dot{E}_{b/c} + \dot{E}_{land}$ where

$\dot{E}_{m/p} = \frac{m\sigma_o}{\sqrt{3}} \int_0^{\gamma}\int_0^{\beta} |V_z(x, y, z)| dxdy$; where

$$V_z(x,y,z) = -z\left[\frac{\partial}{\partial x}V_x(x,y) + \frac{\partial}{\partial y}V_y(y)\right] \qquad (17)$$

$$\dot{E}_{b/c} = \frac{2m\sigma_o}{\sqrt{3}}\left[\int_0^{(H_o - y')}\int_0^{\alpha} |V_y(y)| dxdz + \int_0^{(H_o - y')}\int_0^{b} |V_y(y)| dzdy\right] \qquad (18)$$

$$\dot{E}_{land} = \frac{2m\sigma_o}{\sqrt{3}}\left[\int_0^{a}\int_0^{l} |V_y(y)| dydz + \int_0^{b}\int_0^{l} |V_y(y)| dxdz\right] \qquad (19)$$

where

$$V_y(y) = \frac{y}{H_o - y'} \cdot \frac{V_o \int_0^{x_f(0)} z_s(x,y)dx}{\int_0^{x_f(y)} z_s(x,y)dx} \qquad (20)$$

where γ and β are the limits of integration in x and y axes, l is the die land length, a and b are die opening section lengths in x and y axes and y/ current billet height to die surface. H_o = billet height.

5. SHAPE AND DIMENSIONS OF EXTRUDED PROFILES

Using square billets, the frictional powers at the die land region, for T- and I- sections are evaluated from expressions such as:

i) For T- section shape~

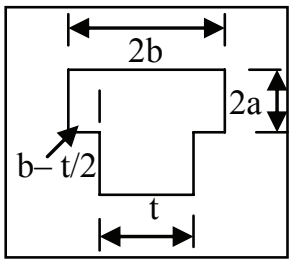

Fig. 2. *T-die opening*

$$\dot{E}_{land} = \frac{2m\sigma_o}{\sqrt{3}}\left[\int_0^{2b}\int_0^{l} V_y(y)dxdz + \int_0^{l}\int_0^{a'} V_y(y)dydz\right] \qquad (21)$$

where $a' = 2a + c$

ii) For I-die opening section shape

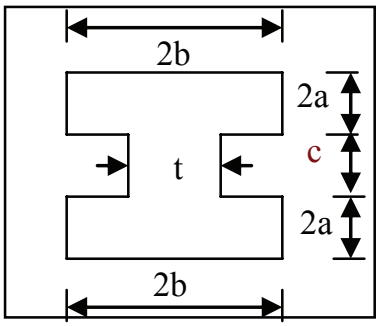

Fig. 3. *I-die opening*

$$E_{f_{land}} = \frac{2m\sigma_o}{\sqrt{3}}\left[\int_0^{l}\int_0^{b'} V_y(y)dxdz + \int_0^{l}\int_0^{a''} V_y(y)dydz\right] \qquad (22)$$

where $b' = 2b + 2b - t = 4b + t$ and $a'' = 4a + c$

6. COMPUTATIONAL METHOD

The area and volume integrals of equations (15-19 and 14 respectively) were performed, using the Gaussian quadrature integration techniques by transforming the polynomial variable by:

$$\phi(x_i) = \frac{(b-a)z_i + (b-a)}{2} \qquad (23)$$

where a and b are respectively the upper and lower limits of integrations of the zone of die surface expressed by $z_s(x, y)$.

The area integrals of the friction losses, $\sum_{i}^{j}\dot{E}_f$ and shear losses, $\sum_{i}^{j}\dot{E}_s$ were computed using the relation

$$\int\int\psi(\eta,\varepsilon)d\eta d\varepsilon = \sum_{1=1}^{m}\sum_{j=i}^{n}W_p\ W_j\ \psi(\eta_i,\varepsilon_j)d\eta d\varepsilon \tag{24}$$

where $\psi(\eta_i,\varepsilon_j)$ is the resultant velocity field and W_p W_j are assigned weightings or integration weight factors, m, n, k are the integration points. And for volume integrals, the internal powers of deformation (W_i) is given as

$$\iiint\psi(\eta,\varepsilon,G)d\eta d\varepsilon dG = \sum_{i=1}^{m}\sum_{j=1}^{n}\sum_{k=1}^{k}\psi(\eta_{i,}\varepsilon_{j,}G_k)dv \tag{25}$$

where $\psi(\eta_i,\varepsilon_j,G_k)$ is the resultant strain and volume under deformation. A computer program written in C++ language was used (Ajiboye, 2006) to evaluate various components of equations (13) to determine dimensionless extrusion pressure J/σ_0, as follows: The dimensionless extrusion pressure $\frac{J^*}{\sigma_0}$ is given by

$$\frac{J^*}{\sigma_0} = \frac{J^*}{A_0V_0\sigma_o} \tag{26}$$

7. RESULTS AND DISCUSSION

7.1. Relative extrusion pressure, (P/Y), determinations

7.1.1. I and T sections openings

Figures 4 and 5 show ypical plots of relative extrusion pressures, P/Y, versus relative die length, l/x_o, computed for different area ratios, A_2/A_1, using a reduction in area of 58% for the T- and I-shaped sections at a given die land length of 15 mm. It can be seen from these figures that, for a given area ratio, the relative extrusion pressures, P/Y, decreases with increasing relative die lengths, l/x_o, to a minimum value at a known relative length. Beyond this relative length, increasing the relative die lengths, l/x_o, lead to increasing relative extrusion pressures, P/Y. The relative die length that produced minimum relative extrusion pressures, P_{min}/Y, gives the optimal relative extrusion pressure for a given area ratio and for a given die land length of 15 mm. or normalized extrusion pressure, P_{min}/Y, at a given area ratio A_2/A_1 = 0.45 for the given die land length of 15 mm considered.

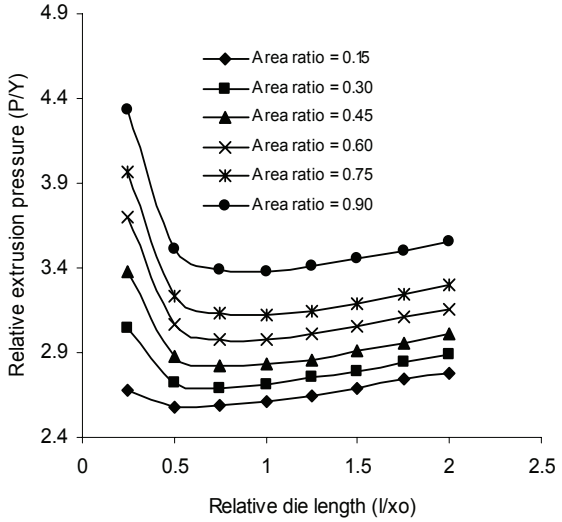

Fig. 4. *Typical effects of area ratios on the extrusion pressures of T-die opening*

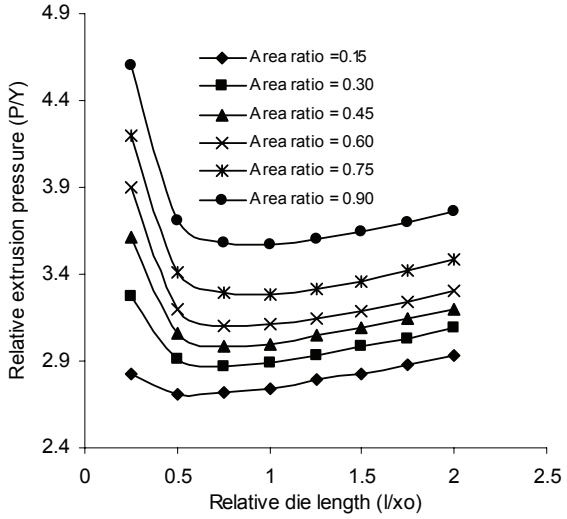

Fig. 5. *Typical effects of area ratios on the extrusion pressures of I-die opening.*

Figures 6 and 7 reveal that, optimal relative extrusion pressures, P_{min}/Y, decrease with increasing area ratios, until a minimum value is reached at a known area ratio. Beyond this area ratio, increasing area ratios cause increasing optimal relative extrusion pressures P_{min}/Y obtained from the relative die length, l/r_o, for a given die land length of 15 mm of figure 7. The correct optimal relative extrusion pressure, P_{min}/Y, that corresponds to a minimum value obtained at a known area ratio of A_2/A_1 = 0.45, for a given die

land of 15 mm gives the correct optimal extrusion pressure or correct normalized extrusion pressures, $P^{/}/Y$, to extrude lead billet through T- and I-die opening at a given percentage reduction in area (i.e. 58%).

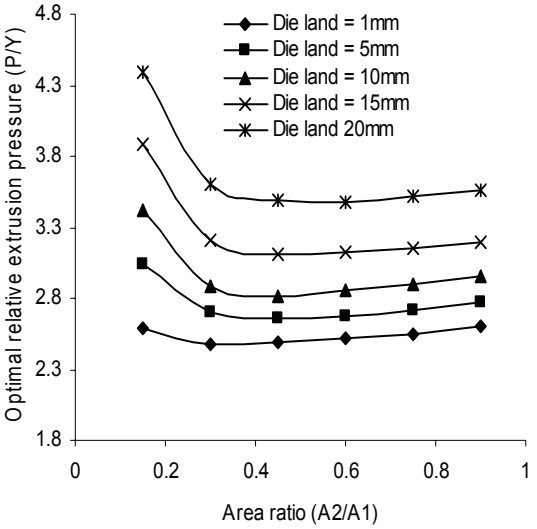

Fig. 6. *Effects of die land lengths on the extrusion pressures of I-shaped section*

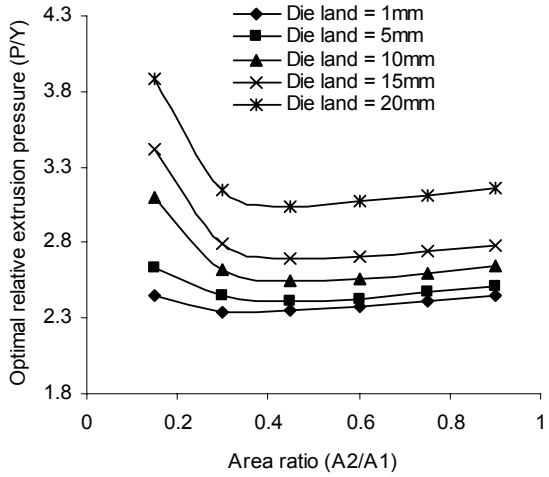

Fig. 7. *Effects of die land lengths on the extrusion pressure of T-shaped section.*

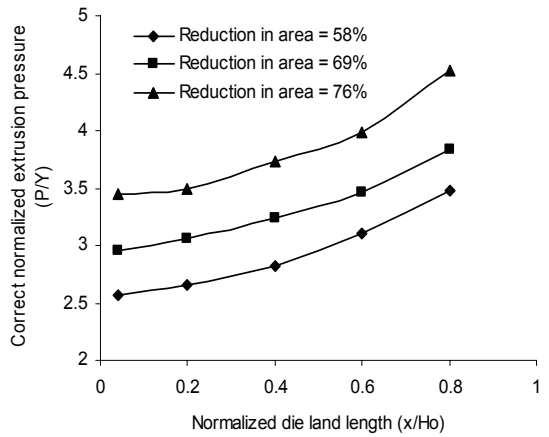

Fig 8. *Typical effects of die reduction in areas on the correct normalized extrusion pressures of I-shaped section*

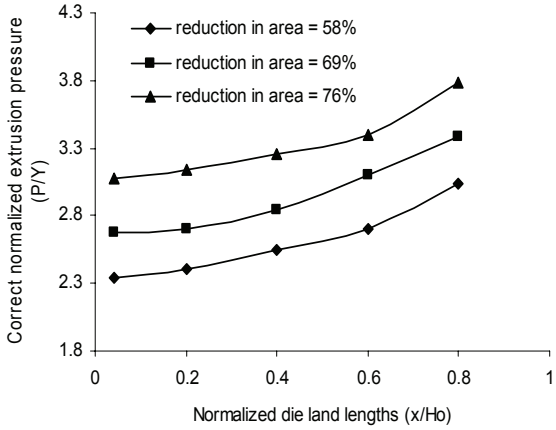

Fig. 9. *Typical effects of die reduction in areas on the correct normalized extrusion pressures of T-shaped section*

7.2. Variation of normalized extrusion pressure with relative die land length

7.2.1. I- and T-section openings

Figures 8 and 9 show typical plots of the correct normalized extrusion pressures, $P^{/}/Y$, against normalized die land lengths at varying die reductions in area indicated for I-shaped and T-shaped sections openings respectively. Similar figures were plotted for rectangular, square and circular die opening geometries. These figures indicate that the correct normalized extrusion pressure is found to increase with increasing percentage die reduction in area at any given die land lengths and also with increasing die land lengths at any given percentage reduction in area. Extrapolating each typical plot of figures 8 and 9 and the likes, to intercept the extrusion pressure axis, give the values of normalized extrusion pressure P_o/Y corresponding to zero die land length for each reduction in area indicated (see table 1).

7.2.2. Die land length and die geometries extrusion pressure contributions, $\Delta P_o/Y$,

For each given reduction in area, this value subtracted from the correct normalized extrusion pressure value $P^{/}/Y$ obtained for various die land lengths gives the extrusion pressure contribution of each die land length to the extrusion pressure as $\Delta P_o/Y = (P^{/} - P_o)/Y$. The dimensionless die land length extrusion pressure contributions, $\Delta P_o/Y$, is seen to generally increase with increase die land lengths and also increase with increase percentages reductions in area (see table 1) for all die openings geometries investigated. It can be seen that, generally, die land lengths contribute significantly to the extrusion pressures for

Table 1. *Die land extrusion pressure contributions, $\Delta P_o/Y$, at various percentages reductions in area for various die openings profiles*

Die opening geometry	% reduction in area, R	Extrapolated extrusion pressure (P_o/Y) MNm^{-2}	Die land length contribution to extrusion pressure $\Delta P_o/Y$				
			1 mm	5 mm	10 mm	15 mm	20 mm
Square	58	1.40	0.03	0.08	0.13	0.18	0.23
	69	1.86	0.04	0.11	0.18	0.25	0.32
	76	1.98	0.04	0.13	0.22	0.31	0.40
Circular	58	1.61	0.03	0.08	0.12	0.17	0.22
	69	1.98	0.04	0.11	0.18	0.25	0.32
	76	2.18	0.04	0.13	0.24	0.37	0.46
Rectangular	58	2.14	0.04	0.09	0.17	0.24	0.31
	69	2.40	0.09	0.19	0.30	0.40	0.51
	76	2.58	0.08	0.21	0.34	0.48	0.61
T-shaped	58	2.30	0.04	0.11	0.25	0.40	0.74
	69	2.42	0.04	0.12	0.27	0.43	0.78
	76	3.01	0.07	0.14	0.30	0.51	0.81
I-shaped	58	2.51	0.05	0.15	0.31	0.60	0.97
	69	2.90	0.05	0.16	0.34	0.65	1.1
	76	3.40	0.06	0.18	0.37	0.72	1.45

all die openings geometries especially at higher die reductions and in particular for I- and T-die opening geometries. Higher perimeters of these geometries coupled with higher frictional effects may possibly account for the higher contributions of die land lengths to the total extrusion pressures (see Table 1).

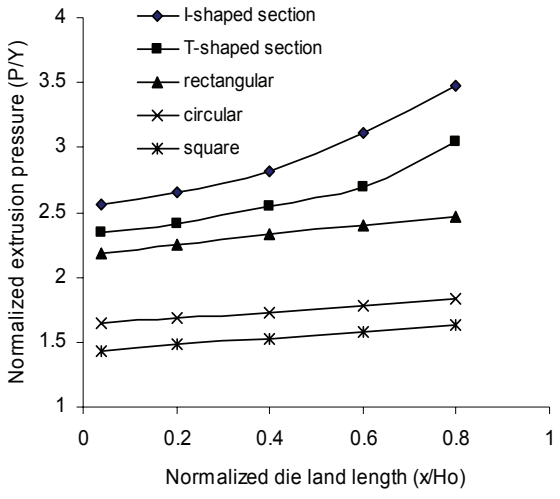

Fig. 10. *Effect of die opening shape on the optimal relative extrusion pressure at a given die reduction in area of 58%*

Figure 10 shows the plot of the correct relative extrusion pressure, P/Y versus increasing relative die land lengths at a given die reduction of 58% for circular, rectangle, square, T and I-sections shaped die openings. The I-shaped section die opening gives the highest extrusion pressure, followed by T-shaped section, rectangular, circular shaped die openings with square section die opening, giving the least extrusion pressure for the given 58% die reduction at any given die land lengths.

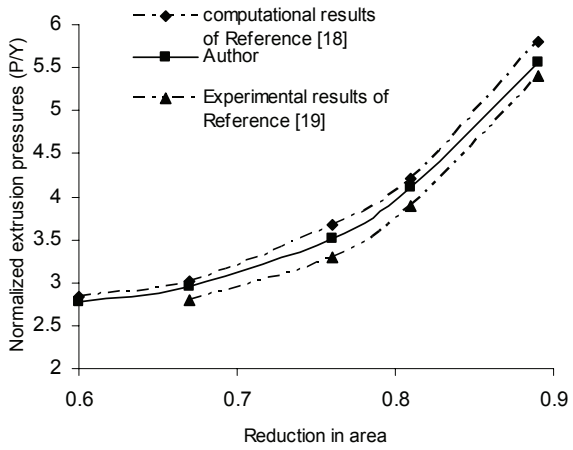

Fig. 11. *Comparison of the average extrusion pressures in the extrusion of I-shaped section with other works in literatures.*

7.3. Comparison with other works in literatures

Figure 11 shows the comparison of the average extrusion pressures computed in this study with other relevant works in literatures (Kar & Das, 1997; Chitkara & Adeyemi, 1977). It is seen that there is good agreement between the present author and others in literatures. The higher values obtained in the present work compared to the experimental results of Chitkara and Adeyemi (1977) is, probably, due to the fact that the present work gives upper bound results. The close agreement between the present results and the computed results of Kar and Das (1997) give further support to the present model.

8. CONCLUSION

Using square or rectangular billets and upper bound analysis, the effect of the die land lengths on the extrusion pressure is formulated in Cartesian coordinates system for complex extruded sections such as square, rectangular, I- and T-shaped sections with power of deformation due to ironing effect at die land included. The extrusion pressure contributions due to the die land evaluated theoretically for shaped sections considered are found to increase with die land lengths for any given percentage reduction and also increase with increasing percentage die reductions at any given die land length. The effect of die land length on the extrusion pressure increases with increasing complexity of die openings geometry with I-shaped section giving the highest

extrusion pressure followed by T-shaped section, rectangular, circular shaped die openings with square section die opening, giving the least extrusion pressure for any die reductions at any given die land lengths. Comparison of the least upper bounds computed with the experimental results and SERR analysis shows that the upper bound method predicts reasonable extrusion loads well within engineering accuracy.

ACKNOWLEDGMENT

The author is deeply indebted to Professor M.B. Adeyemi whose invaluable contribution has made this research an immense success.

REFERENCES

Abrinia, K., Makaremi, M., 2008, A new three-dimensional solution for the extrusion of sections with larger dimensions than the initial, *J. Mat. Proc. Techn*., 205, 1-3, 259-271.

Ajiboye, J.S., 2006, *Extrusion Pressure and Temperature changes during forward Extrusion Process*, PhD thesis, University of Ilorin, Nigeria.

Ajiboye, J.S., Adeyemi, M.B., 2006, Effects of Die land on the cold extrusion of lead alloy, *J. Mat. Proc. Techn.*, 171, 428-436.

Chitkara, N.R, Adeyemi, M.B., 1977, Working pressure and deformation modes in forward extrusion of I and T shaped sections from square slugs, *Proc. 18th Int. MTDR Conf.*, Imperial College of Science and Tech., London, 289-301.

Chitkara, N.R., Celik, K.F., 2001, Extrusion of non-symmetric T-shaped sections an analysis and some experiments, *Int. J. Mech. Sci*, 43, 2961-2987.

Duan, X., Velay, X., Sheppard, T., 2004, Application of finite element method in the hot extrusion of aluminum alloys, *Mat. Sci. Eng*. A, 369, 1-2, 66-75.

Filice, L., Alfaro, I., Gagliardi, F., Cueto, E., Micari, F., Chinesta, F., 2008, A preliminary comparison between finite element and meshless simulations of extrusion, *J. Mat. Proc. Techn*., in Press, Corrected Proof, Available online 18 July 2008.

Kar, P.K., Das, N.S., 1997, Upper bound analysis of extrusion of I-section bars from square/rectangular billets through square dies, *Int. J. Mech. Sci*, 39, 925-934.

Kim, Y.H., Park, J.H., Jin, Y.E., 1999, An analysis of plastic deformation processes for twist-assisted upset forging of cylindrical billets, *Proc. Int. Conf. on Advances in Materials and Processing Technologies (AMPT'99)* and *16th Annual Conference of the Irish Manufacturing Committee (IMC16)*, 1, 79-86.

Kim, Y.H., Park, J.H., Jin, Y.E., Lee, Y., 2000, An analysis of the torsional forming process using the dual stream function, *Proc. 8th Int. Conf. Metal Forming*, eds, Pietrzyk, M., Kusiak, J., Majta, J., Hartley, P., Pillinger, I., A. Balkema, 741-746.

Kiuchi, M., Kish, H., Ishikawa M., 1981, Study on Non symmetric extrusion and drawing, *Int. Journal Mach. Tool, Proc. 22nd Conf. Design and Research*, 523-532.

Kiuchi, M., Yanagimoto, J., Mendoza, V., 1996, Characterization of three-dimensional metal flow in extrusion process, *CIRP Annals - Manufacturing Technology*, 45, 1, 235-238.

Li, G., Jinn, J.T, Wu, W.T., Oh, S.I., 2001, Recent development and applications of three-dimensional finite element modeling in bulk forming processes, *J. Mat. Proc. Techn*., 113, 1-3, 40-45.

Nanhai et al., 2000, Numerical design of die land for shape extrusion, *J. Mat. Proc. Techn*., 101, 81-84.

Sheppard, T., Paterson, S.J., 1982, Some observations on metal flow and the development of structure during the direct and indirect extrusion of commercial purity aluminum, *J. Mech. Work. Techn.*, 7, 1, 39-56.

Sahoo, S.K., Kar, P.K., 2000, Round-to-hexagon drawing through straightly converging dies: an application of the SERR technique, *Int. J. Mech. Sci*., 42, 445-449.

Venkata Reddy, N., Dixit, P. M., Lal, G.K., 1995, Die design for axisymmetric extrusion, *J. Mat. Proc. Techn.*, 55, 3-4, 331-339.

Wu, C.W, Hsu, R.Q., 2000, Theoretical analysis of extrusion of rectangular, hexagonal and octagonal composite clad rods, *Int. J. Mech. Sci*, 42, 473-486.

Yang, D.Y, Lee, H.S., 1993, Analysis of Three-Dimensional Deep Drawing by the Energy Method, *Int. J. Mech. Sci.*, 35, 491-516.

ANALIZA PROCESU WYCISKANIA W MATRYCACH O RÓŻNYCH KSZTAŁTACH Z WYKORZYSTANIEM TRÓJWYMIAROWEJ METODY GÓRNEJ OCENY

Streszczenie

W niniejszej pracy zaprezentowano możliwości przewidywania zmian pola ciśnień podczas wyciskania współbieżnego z wykorzystaniem metody górnej oceny. Analizie poddano wpływ kształtu matrycy z uwzględnieniem stopnia docisku na ewolucje pola ciśnień podczas wyciskania profili o złożonych przekrojach: kwadratowym, prostokątnym, I oraz T. Badania profili wykazały, że wkład ciśnienia generowanego podczas przejścia przez oczko matrycy zwiększa się wraz ze zwiększeniem się długości oczka dla danego stopnia redukcji przekroju, jak również zwiększa się wraz ze zwiększeniem się stopnia przekroju dla danej długości oczka matrycy. Wpływ długości oczka matrycy na ciśnienie zwiesza się również wraz ze wzrostem skomplikowania przekroju wyrobu. Najwyższy wpływ zaobserwowano dla przekroju typu I a następnie T, prostokątnego oraz kwadratowego. Analiza wyników wykazała istotność doboru kształtu matrycy na osiągniecie wymaganej jakości oraz struktury metalurgicznej wyrobów gotowych. Przeprowadzona analiza porównawcza wyników eksperymentalnych oraz obliczeń wykazała, że metoda górnej oceny przewiduje krytyczne wartości sił z zadowalającą dokładnością dla zastosowań inżynierskich.

Submitted: September 9, 2008
Submitted in a revised form: December 12, 2008
Accepted: December 14, 2008